

Silicon-containing dendritic tris-cyclometalated Ir(III) complex and its electrophosphorescence in a polymer host

Youngmin You,^a Cheng-Guo An,^a Deug-Sang Lee,^b Jang-Joo Kim^a and Soo Young Park^{*a}

Received 4th August 2006, Accepted 3rd October 2006

First published as an Advance Article on the web 25th October 2006

DOI: 10.1039/b611288a

In this paper, we present the synthesis and characterization of a new highly phosphorescent cyclometalated Ir(III) complex with a silane-based dendritic substituent. The Ir(III) complex showed $74 \pm 3\%$ of absolute phosphorescence quantum efficiency in the film state. In addition, efficient electrophosphorescence (32.8 cd A^{-1}) employing an Ir(III) complex–poly(*N*-vinylcarbazole) system device is observed. Study of a series of electroluminescent, spectroscopic, and electrochemical data of the Ir(III) complex and the reference Ir(ppy)₃ reveals superior performance of the new Ir(III) complex.

1 Introduction

Since the pioneering works of Forrest and coworkers, electrophosphorescence from transition metal complexes has attracted ever increasing attention due to the potential applications of such complexes in organic light emitting diodes (OLEDs).^{1,2} The highly efficient intersystem crossing induced by the core metal in transition metal complexes makes it possible to utilize the luminescent triplet exciton in addition to the singlet exciton to achieve an internal quantum efficiency of 100%, which is far superior to the internal quantum efficiency up to 25% that is typically recognized as the higher limit in fluorescence-based OLEDs. Among the phosphorescent transition metal complexes studied to date, Ir(III) complexes are currently receiving special attention because they exhibit the highest phosphorescence quantum efficiencies, relatively short phosphorescence lifetime, and facile color tuning by modification of the ligand structures.^{3–6}

Ir(III) complex-based OLEDs are typically fabricated in a configuration in which the emissive layer is comprised of the phosphorescent Ir(III) complexes doped in a small-molecular or polymeric host. The efficiency of devices based on these host–guest systems is normally limited by phase segregation,⁷ triplet–triplet annihilation,⁸ excimer formation,⁹ and other excited-state intermolecular interactions, all of which become more significant as the concentration of emitting dopants is increased. Thus, to maximize the device efficiency, it is necessary to carry out laborious optimization procedures to optimize the doping ratio and to find the host material that is most compatible with the specific Ir(III) complex. In this regard, new Ir(III) complexes that are unaffected by these undesirable excited-state intermolecular interactions are in strong demand.

One promising solution is to provide ‘site-isolation’ by employing a dendritic architecture in the peripheral surface of

the coordination environment of the emission center.^{10–12} The Burn and Samuel group developed a series of dendritic Ir(III) complexes in this manner. They established that encapsulation of emissive tris-cyclometalated Ir(III) complexes with ethylhexyloxy-terminated *meta*-terphenyl type dendrons successfully controlled the intermolecular interactions, thereby enhancing the phosphorescence efficiency. OLEDs based on dendritic Ir(III) complexes of this type gave a luminous efficiency of 55 cd A^{-1} at 4.5 V for green emission,¹³ an external quantum efficiency of 10.4% at 6.4 V for blue emission,¹⁴ and an external quantum efficiency of 5.7% at a luminance of 80 cd m^{-2} for red emission.¹⁵ In addition to these high device efficiencies, the sterically congested structure as well as the terminal alkyl group of the dendritic Ir(III) complex offered much improved solubility in common polar organic solvents enabling easier device fabrication *via* spin coating. A similar dendritic approach employing the pinene group also showed a high luminous efficiency of 10.5 cd A^{-1} at 6 V .¹⁶ However, although the peripheral alkyl moieties (ethylhexyloxy and pinene functionalities) are beneficial in terms of reducing interactions, they create an insulating periphery that leads to reduced current characteristics with increasing dendrimer generation. This is evident in the observation that the first generation of the tris-cyclometalated Ir(III) complexes with six ethylhexyloxy-terminated *meta*-terphenyl dendrons gave inferior luminous efficiency (47 cd A^{-1} at 4.8 V) compared to that (55 cd A^{-1} at 4.5 V) of the first generation of the Ir(III) complex with three identical dendrons.^{13,17} Although these device efficiencies are sufficient for device application, the opposing effects of a dendritic architecture on device efficiency indicate that high dendrimer generation is not the sole structural requirement for high device efficiency. Thus, a novel dendritic substituent with the optimized (compromised between encapsulation and current characteristics) structure is needed.

Previous studies have shown that arylsilanes such as the triphenylsilyl group provide sufficient steric hindrance to protect typical reactive centers. We therefore hypothesized that the tetrahedral configuration of aryl rings around the silicon atom may provide a similar ‘site-isolation’ effect if

^aSchool of Materials Science & Engineering, Seoul National University, San 56-1, Shillim-Dong, Kwanak-Gu, Seoul 151-744, Korea.

E-mail: parksy@snu.ac.kr; Fax: +82-2-886-8331; Tel: +82-2-880-7479

^bCentral R&D center, Dongwoo FineChem Co., Ltd. 1177, Pyungtaek-Si, Kyunggi-Do, 451-764, Korea

applied as the ligand substituents of the Ir(III) complex. In addition, the highly efficient UV emission of arylsilanes suggests that these moieties should give improved efficiency compared to alkyl substituents in OLED applications.^{18,19} Moreover, the silane moieties are expected to provide high thermal and chemical stability as well as glassy properties when incorporated into Ir(III) complexes.²⁰ In this paper, we describe the design and synthesis of a highly phosphorescent tris-cyclometalated homoleptic Ir(III) complex [Ir(TPSppy)₃] (TPSppy = 2-(4'-(triphenylsilyl)biphenyl-3-yl)pyridine) with a silane-based dendritic substituent. We show that a conventional polymer-based [poly(*N*-vinyl carbazole), PVK] OLED doped with this Ir(III) complex has an unprecedentedly high device efficiency (32.8 cd A⁻¹).

2 Results and discussion

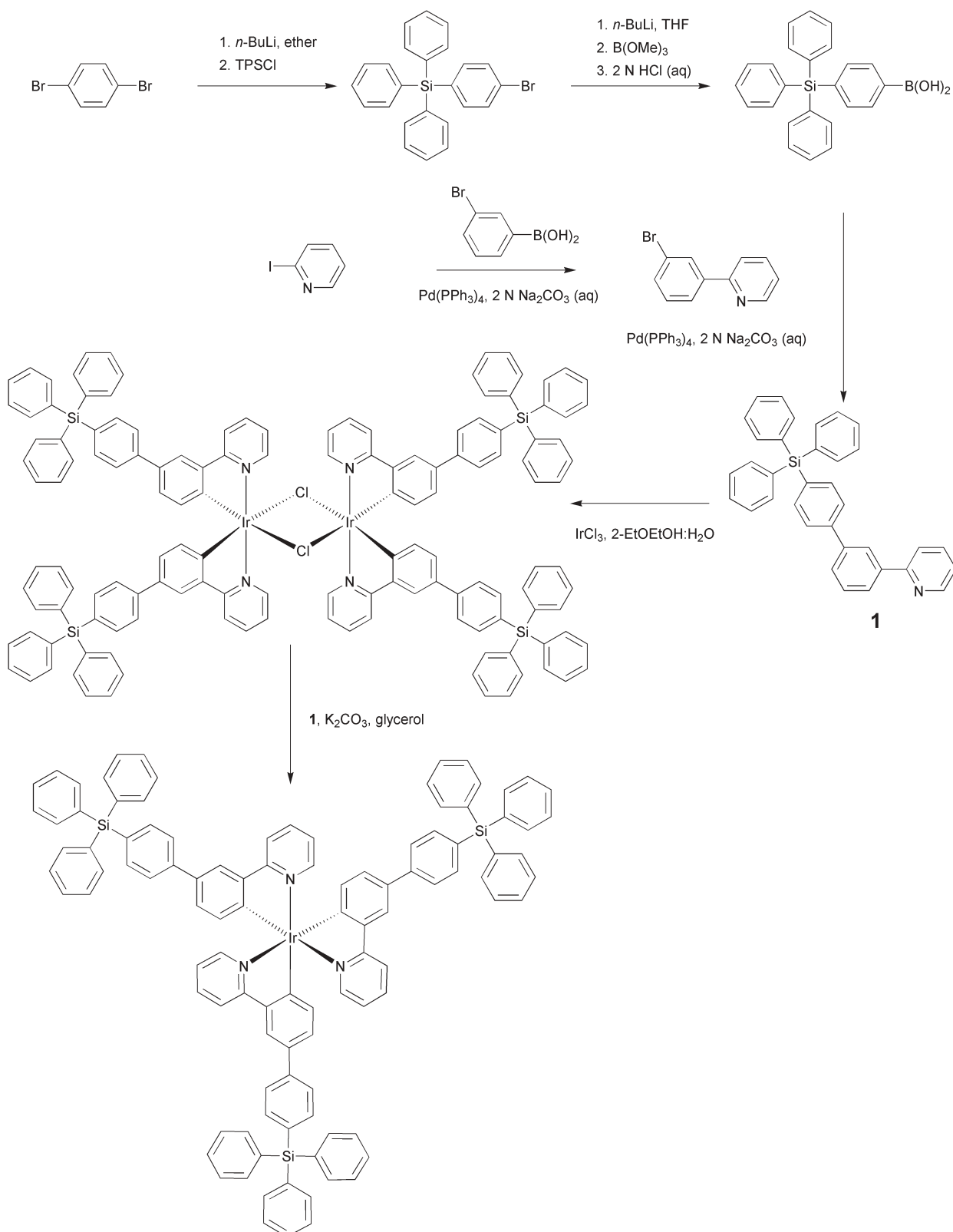
As depicted in Scheme 1, the dendritic arylsilane group in the cyclometalating ligand (**1**) was introduced by a Suzuki–Miyaura coupling reaction of 4-triphenylsilylphenylboronic acid and 2-(3-bromophenyl)pyridine. Nonoyama reaction of this cyclometalating ligand (**1**) and Ir(III) chloride hydrate gave the μ -chloride-bridged dimer in good yield, which was subsequently chelated with **1** in glycerol, affording the tris-cyclometalated homoleptic Ir(III) complex, Ir(TPSppy)₃, in moderate yield. Both Ir(TPSppy)₃ and the μ -chloride-bridged dimer showed excellent solubility in a variety of common organic solvents, demonstrating that the dendritic substituent operated in the coordination environment of the Ir(III) complex. On the other hand, Ir(ppy)₃ (ppy = 2-phenylpyridine), the well-known reference material without dendritic substituents, exhibited relatively poor solubility. From this observation, it was initially anticipated that the severe phase segregation observed in Ir(ppy)₃–PVK films²¹ would be significantly reduced in Ir(TPSppy)₃–PVK films, thereby suppressing the formation of unfavorable low energy traps in OLED devices based on such films.

In the UV-vis absorption spectrum of Ir(TPSppy)₃ (Fig. 1), the metal-to-ligand charge-transfer (MLCT) transition was observed in the region of 370–520 nm along with the ligand-centered $\pi \rightarrow \pi^*$ transitions at 296 nm and 335 nm.²² The spectral shape was similar to that observed for Ir(ppy)₃ except that the spectrum of Ir(TPSppy)₃ contains an additional transition at lower energy (longer than 470 nm), which can be attributed to the extension of the conjugation due to the additional phenyl ring in the phenylpyridine unit of the cyclometalating ligand (**1**). Strong phosphorescent emission of Ir(TPSppy)₃ in solution (1×10^{-5} M in PhMe) as well as in a doped film [3 wt% Ir(TPSppy)₃ in poly(methyl methacrylate) (PMMA)] was observed at 531 nm and 533 nm, respectively (see Table 1). These emission maxima were bathochromically shifted compared to the corresponding values for Ir(ppy)₃, 517 nm for 1×10^{-5} M in PhMe and 515 nm for 3 wt% in PMMA film. Again, this red-shift is attributed to the additional phenyl ring in the cyclometalating ligand. It is noted, however, that the spectra of Ir(TPSppy)₃ and Ir(ppy)₃ have virtually identical shapes, indicating that the same excited and/or ground states were involved in the phosphorescent transitions. In contrast, the dendron part of the triphenylsilyl

group seems to have a negligible effect on the shift of emission maxima, which is further supported by the results of density functional theory (DFT) calculations. As shown in Fig. 2, the distribution of the highest occupied molecular orbital (HOMO) and the lowest unoccupied molecular orbital (LUMO) of Ir(TPSppy)₃ clearly demonstrates the shielding effect of the dendritic substituent. The HOMO is located over the d-orbital of Ir and the biphenyl moiety of the cyclometalating group, whereas the LUMO is located over the pyridine ring. In contrast, the triphenylsilyl dendron exhibits a nearly zero probability of electronic population in the frontier orbitals. Such negligible effect of the triphenylsilyl dendron on the transition in Ir(TPSppy)₃ was also evident in the results of electrochemical measurements. A voltage scan in the range of 1.6 V to –1.5 V (relative to a Ag/Ag⁺ pseudo-reference electrode) for the Ir(TPSppy)₃ and Ir(ppy)₃ solutions containing tetrabutylammonium tetrafluoroborate as a supporting electrolyte showed oxidation at 0.91 V and 0.96 V, respectively. Given the small difference in oxidation potential for Ir(TPSppy)₃ and Ir(ppy)₃, and the fact that the addition of a phenyl ring in the cyclometalating ligand would be expected to change the oxidation potential, the electrochemical findings suggest that the presence of the arylsilane substituents does not notably alter the HOMO energy. Collectively, the results indicate that the triphenylsilyl dendritic substituent plays a key role in shielding the emission center against undesirable non-radiative pathways, without changing the inherent emissive transition of Ir(ppy)₃.

Comparison of the shift in the photoluminescence peaks of Ir(TPSppy)₃ in the solution (531 nm) and film (533 nm) states suggests that the degree of charge-transfer transition (MLCT) is relatively small, ensuring that various host materials with different polarities can be used without altering the emission characteristics. Both solution and solid states of Ir(TPSppy)₃ were highly phosphorescent; the solution phosphorescence quantum yield of Ir(TPSppy)₃ in the Ar-saturated PhMe solution was 0.63, which is higher than that of Ir(ppy)₃ (0.40), and the absolute phosphorescence quantum yield of the film of Ir(TPSppy)₃ was also surprisingly high, reaching $74 \pm 3\%$. These high values can be attributed to the dendritic architecture, which effectively blocks the non-emissive pathways provided by various intermolecular excited-state interactions.

PVK-based OLEDs with the typical configuration of ITO/PSS : PEDOT/PVK : Ir(III) complex/BCP/Alq₃/LiF/Al [ITO = indium tin oxide, PSS = poly(styrene sulfonic acid), PEDOT = poly(3,4-ethylenedioxythiophene), BCP = 2,9-dimethyl-4,7-diphenyl-1,10-phenanthroline, Alq₃ = tris(8-hydroxyquinolinolato)] were fabricated. To investigate the effect of guest concentration, the doping ratio of Ir(III) complex in PVK was varied from 0.5 to 30 wt%. Within this range of doping ratios, we could find the optimum device efficiency (see Table 2). As shown in Fig. 3, none of the electroluminescence spectra of the OLEDs displayed excimer emission at longer wavelengths, indicating that the dendritic substituent in Ir(TPSppy)₃ frustrated the inter-chromophoric interactions at all of the doping ratios tested (0.5–30 wt%).⁹ In addition, the OLED emission characteristics showed no voltage dependence indicating that these OLEDs will give stable emission over long term operation. The peak wavelength in the



Scheme 1 Synthesis of the Ir(III) complex $(\text{Ir}(\text{TPSppy})_3)$.

electroluminescence spectra was 524 nm, which was slightly blue-shifted with respect to that (531 nm) of the photoluminescence spectra. The small shoulder at 450 nm observed in the electroluminescence spectrum of the 0.5 wt% device is attributed

to exciplex formation between the host (PVK) and hole-blocking BCP originating from redundant excitons that could not be trapped by the Ir(III) complex.²³ This small exciplex band was not observed in the spectra of OLEDs with doping ratios of 1 wt% and

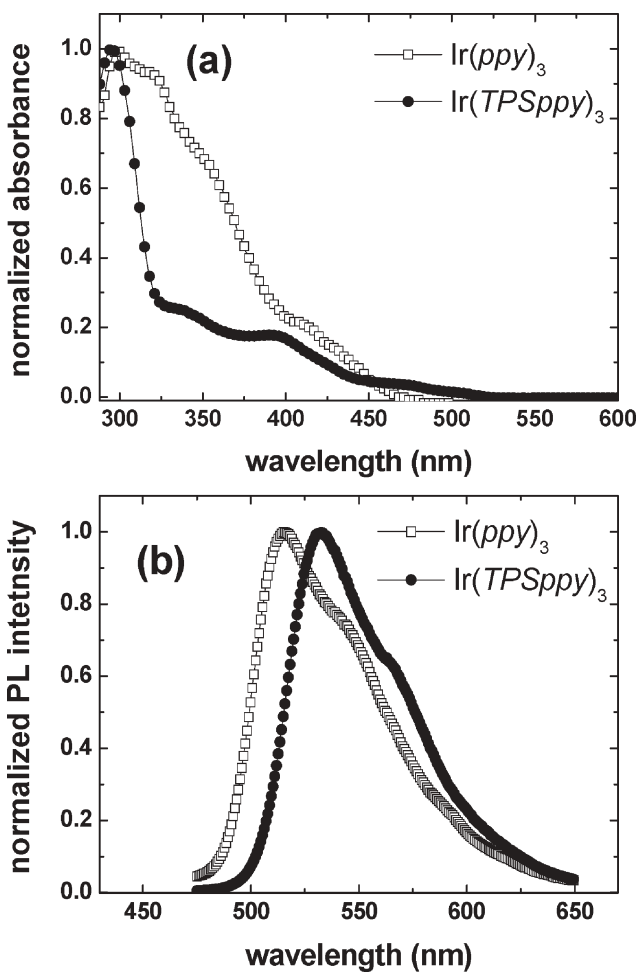


Fig. 1 UV-vis absorption (a) and photoluminescence (b) spectra of Ir(TPSppy)₃ and the reference Ir(ppy)₃ in the solution state (1.0×10^{-5} M in Ar-saturated PhMe).

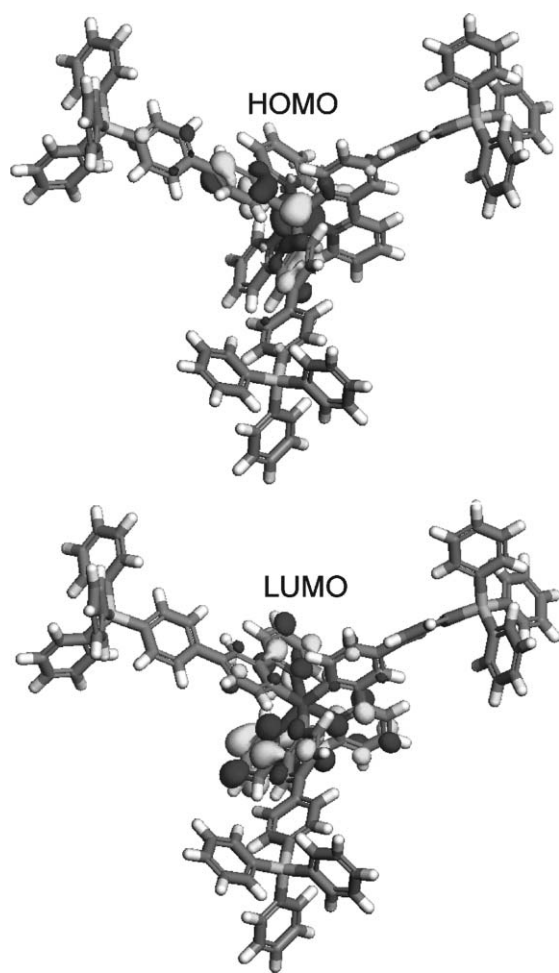


Fig. 2 Calculated contour plots of frontier orbitals of Ir(TPSppy)₃.

Table 1 Physical characterization of Ir(TPSppy)₃ and the reference Ir(ppy)₃

	Absorption wavelength/nm ^a (log ε)	Emission wavelength/nm ^b	E_{ox}/V^c	$E_{\text{red}}/\text{V}^c$	Φ^d
Ir(ppy) ₃	299 (4.08), 320 (4.05), 408 (3.41), 430 (3.20)	517, 515	0.96 ^e , 1.41 ^e	-0.71 ^f	0.40
Ir(TPSppy) ₃	296 (4.98), 335 (4.35), 395 (4.23), 471 (3.54)	531, 533	0.91 ^e , 1.43 ^f	-0.64 ^f	0.63

^a 1.0×10^{-5} M in Ar-saturated PhMe. ^b Solution state, ^a film state (3 wt% Ir(III) complex in PMMA). ^c Determined by cyclic voltammetry (vs. Ag⁺/Ag). ^d Relative phosphorescence quantum yield in solution state. ^e Reversible potential. ^f Irreversible potential.

Table 2 Electroluminescent characteristics of polymer-based devices with Ir(TPSppy)₃ and Ir(ppy)₃

Doped ratio (wt%)	Operating voltage/V at $J^a = 10 \text{ mA cm}^{-2}$, 70 mA cm^{-2}	Maximum luminance/cd m ⁻² (corresponding J)	Maximum luminous efficiency (η)/cd A ⁻¹ (corresponding J)	Maximum power efficiency (η_p)/lm W ⁻¹ (corresponding J)
0.5	8.9, 10.7	2036 (216.4)	5.23 (0.24)	2.52 (0.24)
1	9.4, 11.1	3459 (163.6)	18.3 (0.085)	9.57 (0.085)
4	10.3, 12.0	5665 (71.4)	29.4 (0.061)	15.4 (0.061)
5	10.6, 12.5	9769 (168.7)	25.6 (0.023)	13.4 (0.023)
7	9.8, 11.7	7054 (88.7)	30.8 (0.047)	17.6 (0.047)
10	9.8, 12.0	7215 (71.3)	32.8 (0.057)	18.7 (0.057)
15	10.3, 12.8	13440 (170.2)	28.7 (0.078)	15.0 (0.078)
25	9.4, 12.0	21250 (336.1)	23.5 (0.35)	12.6 (0.11)
30	9.2, 11.9	21250 (355.9)	19.0 (1.58)	10.1 (0.15)
6 ^b	10.4, 12.5	9432 (147.6)	26.4 (0.17)	12.7 (0.17)

^a Current density (mA cm^{-2}). ^b Reference device (ITO/PEDOT : PSS/PVK : Ir(ppy)₃/BCP/Alq₃/LiF/Al), only optimized values are shown.

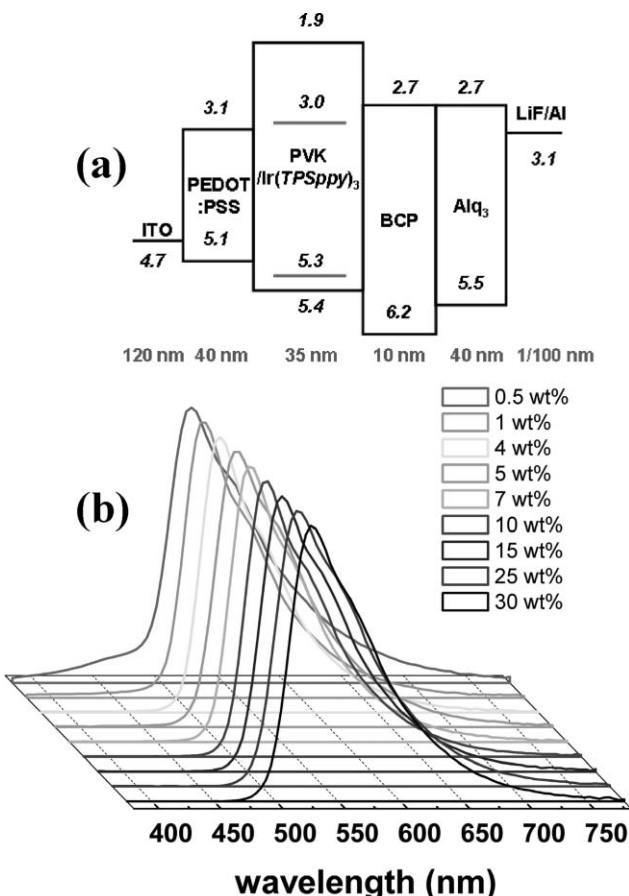


Fig. 3 (a) A configuration of the polymer-based OLED (numbers represent the energy value in eV units). (b) Normalized electroluminescence spectra of devices with different doping ratios (wt% relative to PVK) of Ir(TPSppy)₃.

higher, indicating effective entrapment of excitons in the Ir(TPSppy)₃ in these devices.

The profiles of current density (mA cm^{-2}) as a function of applied voltage [Fig. 4(a)] show that the turn on voltage of the device decreased with increasing doping ratio. If we consider the energy level of Ir(TPSppy)₃ [Fig. 3(a)], it is likely that the high doping ratio enables favorable balanced charge-transfer within the polymer layer; specifically, increase of the content of Ir(III) complex may facilitate transfer of the electron along the Ir(III) complex *via* a hopping mechanism.¹⁹

A maximum luminous efficiency of 32.8 cd A^{-1} was recorded at 5.5 V from the device with 10 wt% Ir(TPSppy)₃ whereas that of Ir(ppy)₃ was 26.4 cd A^{-1} at 6.5 V from a device with 6 wt% doped ratio with an identical device configuration [see Fig. 4(c)]. [For Ir(ppy)₃-based devices, only the best result (6 wt%) is included.] In addition, the maximum power efficiency of the Ir(TPSppy)₃ device was 18.7 lm W^{-1} , whereas that of the Ir(ppy)₃ device was 10.9 lm W^{-1} . If we consider that Ir(TPSppy)₃ has a higher molecular weight than Ir(ppy)₃ (1658.74 vs. 654.78, respectively), we find that the optimized doping ratio of Ir(TPSppy)₃ (10 wt%) in fact corresponds to a smaller molar content than that of Ir(ppy)₃ (6 wt%). Thus we can conclude that the higher efficiency of Ir(TPSppy)₃ compared to Ir(ppy)₃ is due to its inherent high

phosphorescence quantum efficiency rather than simply to the ‘site-isolation’ under electrical excitation (*i.e.* triplet–triplet annihilation) provided by dendritic structures. As shown in Fig. 4(c), the maximum luminous efficiency for both Ir(TPSppy)₃ and Ir(ppy)₃ appears at low current density and drops slowly with increasing current density. However, the luminous efficiencies of Ir(TPSppy)₃-based devices are generally higher than those of Ir(ppy)₃-based devices. Increasing the doping ratio of Ir(TPSppy)₃ three-fold, from 10 wt% to 30 wt%, caused the maximum luminous efficiency to change from 32.8 cd A^{-1} to 19.0 cd A^{-1} , a decrease that was smaller than the decrease obtained by changing the doping ratio in the Ir(ppy)₃-based device. In fact, the luminous efficiency of Ir(ppy)₃ showed a strong dependence on the doping ratio, decreasing from 26.4 cd A^{-1} to 15 cd A^{-1} when the doping ratio was increased 1.5-fold from 6 wt% for 9 wt% Ir(ppy)₃, and then sharply decreasing on further increase of the Ir(ppy)₃ content. In addition, roll-off in luminous efficiency at high current density, most probably due to triplet–triplet annihilation, was significantly less for Ir(TPSppy)₃ than for Ir(ppy)₃. The present results thus indicate that excited-state intermolecular interactions were suppressed even in the heavily doped system of Ir(TPSppy)₃. It is worth noting that the luminous efficiency of the Ir(TPSppy)₃ device (32.8 cd A^{-1}) is the highest value ever achieved among polymer-based OLEDs employing unblended (*i.e.* without electron transporting materials such as 2-(4-biphenyl)-5-(4-*tert*-butylphenyl)-1,3,4-oxadiazole (PBD) or 1,3-bis(5-(4-*tert*-butylphenyl))-1,3,4-oxadiazole (OXD-7)) PVK as a host.^{24,25} Furthermore, considering that this luminous efficiency was achieved in a standard multilayered polymer device, our results indicate that Ir(TPSppy)₃ outperforms previously reported Ir(III) complexes.

3 Conclusions

In summary, we successfully synthesized a new highly phosphorescent tris-cyclometalated homoleptic Ir(III) complex [Ir(TPSppy)₃] with a silane-based dendritic substituent. The Ir(III) complex showed efficient phosphorescence of $74 \pm 3\%$ absolute phosphorescent quantum yield in the solid state. The maximum luminous efficiency of polymer-based light emitting diodes employing Ir(TPSppy)₃ reached 32.8 cd A^{-1} , which was superior to that achieved using Ir(ppy)₃ in a device with an identical configuration.

4 Experimental

Synthesis of 4-bromo-triphenylsilylbenzene

After a magnetically stirred solution of *p*-dibromobenzene (24.0 g, 101 mmol) in anhydrous ether (200 mL) was cooled down to -78°C , 64.9 mL of *n*-BuLi (1.6 M in hexane, 101 mmol) was added slowly under nitrogen. After 1 h, the reaction mixture was warmed to room temperature and stirred for an additional 1 h. Then, triphenylsilylchloride (25.0 g, 84.8 mmol) was delivered dropwise *via* syringe. After 2 h, the solution was poured into 400 mL of water and the crude product was extracted with excess ether. Reprecipitation with THF and MeOH gave a white powder in 43% yield (15.1 g, 36.4 mmol). ¹H NMR (CDCl_3 , 500 MHz): δ 7.37 (m, 6H),

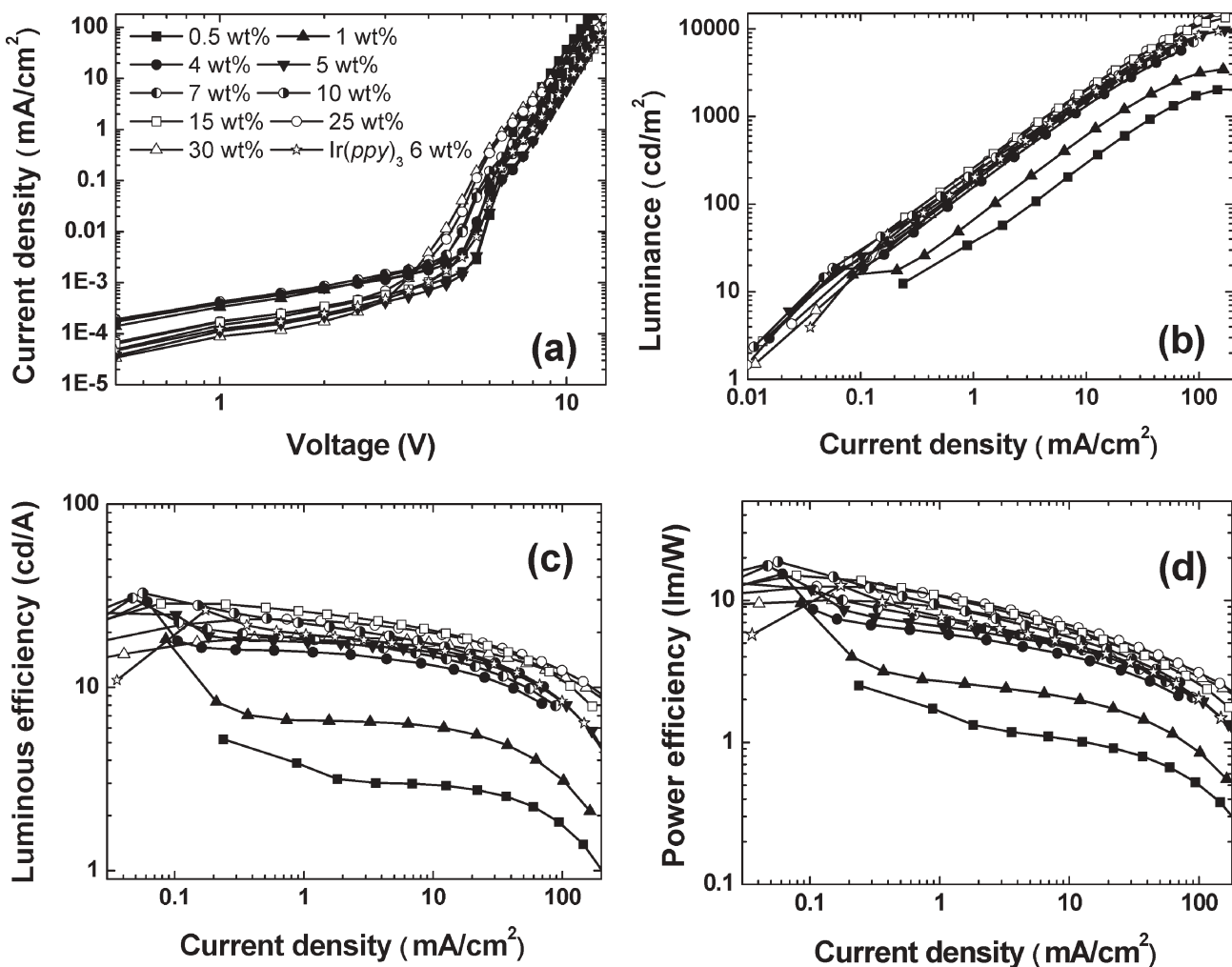


Fig. 4 Plots of (a) current density (mA cm^{-2}) vs. voltage (V), (b) luminance (cd m^{-2}), (c) luminous efficiency (cd A^{-1}), and (d) power efficiency (lm W^{-1}) vs. current density (mA cm^{-2}) of the fabricated devices.

7.43 (m, 3H), 7.50 (d, $J = 8.0 \text{ Hz}$, 2H), 7.54 (d, $J = 7.7 \text{ Hz}$, 6H), 7.57 (d, $J = 7.7 \text{ Hz}$, 2H). ^{13}C NMR (CDCl_3 , 125 MHz): δ 128.1, 128.2, 129.5, 129.8, 131.3, 136.5, 136.6, 138.1.

Synthesis of 4-triphenylsilylphenylboronic acid

To a magnetically stirred solution of 4-bromo-triphenylsilylbenzene (13.7 g, 33.2 mmol) in 200 mL of anhydrous THF, 33.2 mL of *n*-BuLi (1.6 M in hexane, 53.1 mmol) was added *via* syringe under nitrogen at -78°C . After stirring for 1 h, 10 mL (53.1 mmol) of trimethylborate was inserted to a reaction vessel slowly for 10 min. Then the temperature of the reaction mixture was raised to room temperature, and stirring for an additional 2 h was carried out. Finally the reaction mixture was poured into 200 mL of water and acidified with aqueous 2 M HCl. The crude product was extracted with EtOAc and purified by silica gel column chromatography (*n*-hexane : EtOAc = 9 : 1) to give a white powder in 40% yield (5.1 g, 13.4 mmol). ^1H NMR (CDCl_3 , 300 MHz): δ 7.40 (m, 11H), 7.57 (m, 7H), 7.71 (d, $J = 8.0 \text{ Hz}$, 2H), 8.18 (d, $J = 8.0 \text{ Hz}$, 1H). ^{13}C NMR (CDCl_3 , 125 MHz): δ 128.2, 134.1, 134.9, 136.1, 136.6, 136.7, 140.1. GC-MS (EI) m/z 380 (M^+), 249. Anal. Calcd for $\text{C}_{24}\text{H}_{21}\text{BO}_2\text{Si}$: C, 75.79; H, 5.57. Found: C, 75.76; H, 5.90%.

Synthesis of 2-(3-bromophenyl)pyridine

2-Iodopyridine (3.89 g, 19.0 mmol), 3-bromophenylboronic acid (3.81 g, 19.0 mmol), and tetrakis(triphenylphosphine)palladium(0) (0.66 g, 0.57 mmol) were added to a round-bottomed flask equipped with a reflux condenser and dissolved in 200 mL of THF. After adding 100 mL of aqueous 2 M sodium carbonate solution, the reaction mixture was heated at 80°C for 1 d. The cooled crude mixture was poured onto water and extracted with CH_2Cl_2 and dried over anhydrous magnesium sulfate. Finally, silica gel column purification (*n*-hexane : EtOAc = 5 : 1) gave a sticky liquid (3.43 g, 14.7 mmol) in 77% yield. ^1H NMR (CDCl_3 , 300 MHz): δ 7.28 (m, 4H), 7.73 (d, $J = 7.1 \text{ Hz}$, 2H), 8.38 (m, 2H). ^{13}C NMR (CDCl_3 , 125 MHz): δ 118.0, 122.7, 122.8, 131.5, 134.6, 134.7, 137.4, 141.0, 150.4, 155.2. Direct injection probe (DIP)-MS (FAB) m/z 233 (M^+), 154.

Synthesis of the cyclometalating ligand 1

The same procedure as for 2-(3-bromophenyl)pyridine was applied to give a yellow powder (1.12 g, 2.29 mmol) in 41% yield. ^1H NMR (300 MHz, CDCl_3): δ 7.25 (m, 2H), 7.40 (m, 11H), 7.60 (m, 6H), 7.68 (d, $J = 8.3 \text{ Hz}$, 2H), 7.74 (m, 2H), 7.99

(d, $J = 6.5$ Hz, 2H), 8.42 (s, 1H), 8.70 (td, $J = 4.7$ Hz, 1H). ^{13}C NMR (CDCl_3 , 125 MHz): δ 121.0, 122.5, 126.5, 128.0, 128.1, 129.7, 129.9, 134.3, 135.4, 136.6, 137.0, 137.1, 138.3, 140.7, 150.0, 157.6. DIP-MS (FAB) m/z 489 (M^+), 414, 336, 259, 154. Anal. Calcd for $\text{C}_{35}\text{H}_{27}\text{NSi}$: C, 85.85; H, 5.56; N, 2.86. Found: C, 85.94; H, 5.64; N, 3.09%

Synthesis of μ -chloride-Ir(III) dimer

Literature procedure²⁶ was applied (40% yield). ^1H NMR (500 MHz, CDCl_3): δ 6.06 (s, 4H), 6.25 (t, 4H), 6.95 (d, $J = 7.6$ Hz, 4H), 7.18 (m, 28H), 7.25 (m, 28H), 7.31 (t, $J = 8.5$ Hz, 20H), 7.39 (d, $J = 7.7$ Hz, 6H), 7.59 (d, $J = 8.0$ Hz, 6H), 9.00 (d, $J = 5.5$ Hz, 4H). ^{13}C NMR (CDCl_3 , 125 MHz): δ 118.5, 122.3, 122.8, 126.5, 127.7, 128.1, 129.2, 129.3, 134.8, 136.1, 136.6, 137.1, 138.7, 144.4, 145.2, 151.4, 168.0. HRMS (FAB) calculated M^+ 1216.0509; observed M^+ 1216.0499. Anal. Calcd for $\text{C}_{140}\text{H}_{104}\text{Cl}_2\text{Ir}_2\text{N}_4\text{Si}_4$: C, 69.77; H, 4.35; N, 2.32. Found: C, 69.61; H, 4.64; N, 2.46%

Synthesis of tris-cyclometalated Ir(III) complex [$\text{Ir}(\text{TPSpp})_3$]

Literature procedure²⁶ was applied (48% yield). ^1H NMR (300 MHz, CDCl_3): δ 6.90–7.02 (m, 16H), 7.07–7.23 (m, 17H), 7.32–7.43 (m, 21H), 7.51–7.68 (m, 20H), 7.78–7.92 (m, 4H). ^{13}C NMR (CDCl_3 , 125 MHz): δ 119.0, 120.0, 122.1, 124.1, 130.1, 136.1, 137.3, 143.9, 147.3, 161.4, 167.0. DIP-MS (FAB) m/z 1658 (M^+), 1581, 1506, 1430, 1093, 1017, 259. Anal. Calcd for $\text{C}_{105}\text{H}_{78}\text{IrN}_3\text{Si}_3$: C, 76.05; H, 4.74; N, 2.53. Found: C, 76.08; H, 5.01; N, 2.67%

Characterization and device fabrication

Absorption spectra of solutions (1.0×10^{-5} M in PhMe) were recorded with SHIMADZU UV-1650PC from 280 to 700 nm. Photoluminescence (PL) spectra were obtained with a SHIMADZU RF-5301PC spectrophotometer in the range of ca. 400–700 nm. Absorption and PL spectra of Ir(III) complexes in solution were measured after Ar-saturation. Absolute phosphorescence quantum yields (PLQY) were measured in a system comprising a 6 in integrated sphere. An excitation beam of 325 nm from He : Cd CW laser was loosely focused on the sample, and the emission light was spectrally resolved by using a 30 cm monochromator (Acton) after passing through the sample. The light signal was detected via a photomultiplier tube. Cyclic voltametric experiments were carried out with a model 273A (Princeton Applied Research) using three electrode cell assemblies comprising a quasi Ag wire as a reference electrode and Pt as counter and working electrodes. Measurements were carried out in Ar-saturated dichloromethane solution with tetrabutylammonium tetrafluoroborate (5 mM) as a supporting electrolyte at a scan rate of 50 mV s⁻¹. Each potential was calibrated with ferrocene as a reference. Dmol³ module installed within Materials Studio (Accelrys) was used for DFT calculations. Ground state geometry optimization and single point calculation were done with BLYP functional and DNP basis sets under effective core potential. SCF tolerance was maintained within 10^{-6} . For device fabrication, PEDOT : PSS (Baytron P VP Al 4083 purchased from H. C. Starck) was spin-coated

onto pre-cleaned and UV-O₃ treated ITO (Asahi) substrates, yielding layers with a thickness of ca. 40 nm, then baked at 200 °C for 10 min to remove residual water. PVK (Kanto Chem. Corp.) doped with dyes was spin-coated onto the PEDOT : PSS layer resulting in a layer ca. 35 nm thickness. All of the polymer layers were fabricated in Ar-atmosphere. Small molecules and metals were thermally evaporated at 10^{-7} Torr. Finally, devices were encapsulated in a glove box with a glass cap. Current-density–voltage characteristics were measured with a Keithley 2400 source meter. The brightness and electroluminescence spectra of the devices were measured with SpectraColorimeter PR-650.

Acknowledgements

This work was supported in parts by the Ministry of Science and Technology of Korea through a National Research Laboratory (NRL) program awarded to Prof. Soo Young Park and by Dongwoo FineChem Co., Ltd. Prof. J.-J Kim acknowledges the Ministry of Commerce, Industry and Energy of Korea through the OLED center, Center for Electro- and Photo-Responsive Molecules, and Samsung SDI Corporation for financial support.

References

- M. A. Baldo, D. F. O'Brian, Y. You, A. Shoustikov, S. Sibley, M. E. Thompson and S. R. Forrest, *Nature*, 1998, **395**, 151.
- M. A. Baldo, M. E. Thompson and S. R. Forrest, *Nature*, 2000, **403**, 750.
- M. A. Baldo, S. Lamansky, P. E. Burrows, M. E. Thompson and S. R. Forrest, *Appl. Phys. Lett.*, 1999, **75**, 4.
- M. Ikai, S. Tokito, Y. Sakamoto, T. Suzuki and Y. Taga, *Appl. Phys. Lett.*, 2001, **79**, 156.
- F. C. Chen, Y. Yang, M. E. Thompson and J. Kido, *Appl. Phys. Lett.*, 2002, **80**, 2308.
- M. K. Nazeeruddin, R. Humphry-Baker, D. Berner, S. Rivier, L. Zuppiroli and M. Graetzel, *J. Am. Chem. Soc.*, 2003, **125**, 8790.
- Y. You, S. H. Kim, H. K. Jung and S. Y. Park, *Macromolecules*, 2006, **39**, 349.
- M. A. Baldo, C. Adachi and S. R. Forrest, *Phys. Rev. B*, 2000, **62**, 10967.
- B. D'Andrade, J. Brooks, V. Adamovich, M. E. Thompson and S. R. Forrest, *Adv. Mater.*, 2002, **14**, 1032.
- M. Halim, J. N. G. Pillow, I. D. W. Samuel and P. L. Burn, *Adv. Mater.*, 1999, **11**, 371.
- A. W. Freeman, S. C. Koene, P. R. L. Malenfant, M. E. Thompson and J. M. J. Frechet, *J. Am. Chem. Soc.*, 2000, **122**, 12385.
- E. B. Namdas, A. Ruseckas, I. D. W. Samuel, S.-C. Lo and P. L. Burn, *J. Phys. Chem. B*, 2004, **108**, 1570.
- S.-C. Lo, N. A. H. Male, J. P. J. Markham, S. W. Magennis, P. L. Burn, O. V. Salata and I. D. W. Samuel, *Adv. Mater.*, 2002, **14**, 975.
- S.-C. Lo, G. J. Richards, J. P. J. Markham, E. B. Namdas, S. Sharma, P. L. Burn and I. D. W. Samuel, *Adv. Funct. Mater.*, 2005, **15**, 1451.
- T. D. Anthopoulos, M. J. Frampton, E. B. Namdas, P. L. Burn and I. D. W. Samuel, *Adv. Mater.*, 2004, **16**, 557.
- H. Z. Xie, M. W. Liu, O. Y. Wang, X. H. Zhang, C. S. Lee, L. S. Hung, S. T. Lee, P. F. Teng, H. L. Kwong, H. Zheng and C. M. Che, *Adv. Mater.*, 2001, **13**, 1245.
- S.-C. Lo, T. D. Anthopoulos, E. B. Namdas, P. L. Burn and I. D. W. Samuel, *Adv. Mater.*, 2005, **17**, 1945.
- R. J. Holmes, S. R. Forrest, T. Sajoto, A. Tamayo, P. I. Djurovich, M. E. Thompson, J. Brooks, Y.-J. Tung, B. W. D'Andrade, M. S. Weaver, R. C. Kwong and J. J. Brown, *Appl. Phys. Lett.*, 2005, **87**, 243507.
- X. Ren, J. Li, R. J. Holmes, P. I. Djurovich, S. R. Forrest and M. E. Thompson, *Chem. Mater.*, 2004, **16**, 4743.

- 20 X.-M. Liu, J. Xu, X. Lu and C. He, *Org. Lett.*, 2005, **7**, 2829.
21 Y.-Y. Noh, C.-L. Lee and J.-J. Kim, *J. Chem. Phys.*, 2003, **118**, 2853.
22 A. P. Wilde, K. A. King and R. J. Watts, *J. Phys. Chem.*, 1991, **95**, 629.
23 Y. Wang, F. Teng, Z. Xu, Y. Hou, Y. Wang and X. Xu, *Eur. Polym. J.*, 2005, **41**, 1020.
24 X. Gong, J. C. Ostrowski, G. C. Bazan, D. Moses, A. J. Heeger, M. S. Liu and A. K. Y. Jen, *Adv. Mater.*, 2003, **15**, 45.
25 Y. Kawamura, S. Yanagida and S. R. Forrest, *J. Appl. Phys.*, 2002, **92**, 87.
26 A. B. Tamayo, B. D. Alleyne, P. I. Djurovich, S. Lamansky, I. Tsypa, N. H. Ho, R. Bau and M. E. Thompson, *J. Am. Chem. Soc.*, 2003, **125**, 7377.

Find a SOLUTION

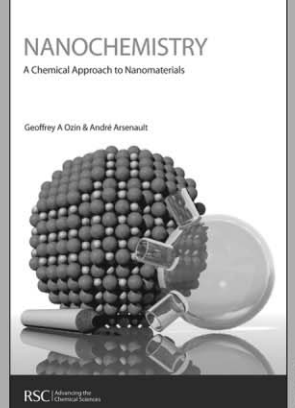
... with books from the RSC

Choose from exciting textbooks, research level books or reference books in a wide range of subject areas, including:

- Biological science
- Food and nutrition
- Materials and nanoscience
- Analytical and environmental sciences
- Organic, inorganic and physical chemistry

Look out for 3 new series coming soon ...

- RSC Nanoscience & Nanotechnology Series
- Issues in Toxicology
- RSC Biomolecular Sciences Series



28040542

RSC | Advancing the
Chemical Sciences

www.rsc.org/books